

# Molecular-Level Manipulation of V<sub>2</sub>O<sub>5</sub>/Polyaniline Layer-by-Layer Films To Control Electrochromogenic and Electrochemical Properties

Fritz Huguenin,<sup>†</sup> Marystela Ferreira,<sup>†</sup> Valtencir Zucolotto,<sup>†</sup> Francisco C. Nart,<sup>‡</sup> Roberto M. Torresi,<sup>§</sup> and Osvaldo N. Oliveira, Jr.<sup>\*,†</sup>

*Instituto de Física de São Carlos, Instituto de Química de São Carlos, and Instituto de Química, Universidade de São Paulo, 13560-970 São Carlos (SP), Brazil*

*Received November 14, 2003. Revised Manuscript Received March 18, 2004*

This work describes how manipulation at the molecular level of V<sub>2</sub>O<sub>5</sub>/polyaniline (PANI) nanocomposites built with the layer-by-layer (LBL) technique promotes enhancement of charge storage capability, new electrochromic effects, and control of ionic flux. By changing the film architecture we control the amount of PANI participating in the redox processes of the LBL films. As a consequence, the films display the electrochemical profile of V<sub>2</sub>O<sub>5</sub> and the chromogenic properties of PANI. Impedance spectroscopy data show the presence of distinct phases in the nanocomposite, which allows a conducting path for the whole potential range between 0.5 and −1.5 V. Further control of the properties of the nanoarchitectures is achieved by adsorbing V<sub>2</sub>O<sub>5</sub>/PANI LBL films onto a cast PANI film. By changing the time of immersion of the PANI–V<sub>2</sub>O<sub>5</sub>/PANI system into a solution of LiClO<sub>4</sub>/propylene carbonate (PC), we were able to monitor the mass gain/loss ( $\Delta m$ ) with an electrochemical quartz crystal microbalance (EQCM) as a function of charge ( $q$ ) and control the intercalating/deintercalating species. The  $\Delta m/q$  ratio shifted from 0.77 to −0.12 mg C<sup>−1</sup> when a 10-bilayer LBL film was immersed into a solution of LiClO<sub>4</sub>/PC during 24 h, indicating a change from an anionic contribution to a cationic one for the charge compensation process. It is envisaged that the molecular-level control demonstrated here may be exploited in producing efficient lithium batteries as well as electrochromic devices and sensors.

## Introduction

Nanocomposites formed from transition metal oxides and electronically conducting polymers (ECP) have been extensively studied, and many recent examples exist of nanohybrids as potential materials for electrochromic devices and lithium secondary batteries. V<sub>2</sub>O<sub>5</sub> and polyaniline (PANI) are important in this context because of their high charge capacity and multicolor properties when they are reduced/oxidized. A synergistic effect has been observed for specific capacity when cathodes are formed from an intimate contact between the oxide and the ECP.<sup>1–5</sup> This optimization is attributed to a gain in the rate of lithium ions within the host matrix and to an increase in electronic conductivity. Mechanical and electrochemical properties of ECP/V<sub>2</sub>O<sub>5</sub> nanocomposites depend on preparation details. Kanatzidis et al. showed

that V<sub>2</sub>O<sub>5</sub> xerogel films exposed to a dispersion containing aniline formed a nanocomposite powder with the PANI intercalated within the interlayer region of V<sub>2</sub>O<sub>5</sub>.<sup>6</sup> In electrochemical experiments, Leroux et al. observed a lower capacity of Li insertion for this nanocomposite (0.60 Li per formula unit) than for V<sub>2</sub>O<sub>5</sub> xerogel (1.05 Li per formula unit).<sup>1,2</sup> The oxidative polymerization of V<sub>2</sub>O<sub>5</sub> promotes the chemical reduction of a fraction of V<sup>5+</sup> sites irreversibly, decreasing the charge capacity of the cathode. However, a postoxidative treatment with O<sub>2</sub> reoxidized V<sub>2</sub>O<sub>5</sub> sites, increasing the capacity of Li insertion (1.35 Li per formula unit). The simultaneous polymerization is another procedure to produce polypyrrole (Ppy)/V<sub>2</sub>O<sub>5</sub> nanocomposites by which nanocomposite aerogel powders were formed with excellent charge capacity (3.8 Li per formula unit).<sup>7</sup> Huguenin et al. employed simultaneous polymerization in forming homogeneous films from various ECP and V<sub>2</sub>O<sub>5</sub>.<sup>5,8</sup> In this case, microcomposites are formed for molar fractions of PANI into V<sub>2</sub>O<sub>5</sub> equal to or greater than 1, and the films are not as homogeneous as those with a smaller amount of PANI.<sup>9</sup> The synthesis of the oxide

\* Corresponding author. E-mail: chu@ifsc.usp.br.

<sup>†</sup> Instituto de Física de São Carlos.

<sup>‡</sup> Instituto de Química de São Carlos.

<sup>§</sup> Instituto de Química.

(1) Leroux, F.; Koene, B. E.; Nazar, L. F. *J. Electrochem. Soc.* **1996**, *143*, L181.

(2) Leroux, F.; Goward, G.; Power, W. P.; Nazar, L. F. *J. Electrochem. Soc.* **1997**, *144*, 3886.

(3) Lira-Cantú, M.; Gómez-Romero, P. *J. Electrochem. Soc.* **1999**, *146*, 2029.

(4) Huguenin, F.; Torresi, R. M.; Buttry, D. A.; Pereira da Silva, J. E.; de Torresi, S. I. C. *Electrochim. Acta* **2001**, *46*, 3555.

(5) Huguenin, F.; Torresi, R. M.; Buttry, D. A. *J. Electrochem. Soc.* **2002**, *149*, A546.

(6) Kanatzidis, M. G.; Wu, C.-G.; Marcy, H. O.; Kannewurf, C. R. *J. Am. Chem. Soc.* **1989**, *111*, 4139.

(7) Wong, H. P.; Dave, B. C.; Leroux, F.; Harreld, J.; Dunn, B.; Nazar, L. F. *J. Mater. Chem.* **1998**, *8*, 1019.

(8) Huguenin, F.; Girotto, E. M.; Torresi, R. M.; Buttry, D. A. *J. Electroanal. Chem.* **2002**, *536*, 37.

(9) Huguenin, F.; Torresi, R. M. *Quim. Nova* (in press).

gel in the presence of a dispersion of preformed Ppy avoids the irreversible reduction of  $V_2O_5$  sites, but Ppy/ $V_2O_5$  nanocomposites cannot be formed. The microcomposites showed a low charge capacity in comparison with that for  $V_2O_5$  xerogel.<sup>2</sup>

In a recent work, Ferreira et al. showed that PANI/ $V_2O_5$  nanocomposites obtained with the layer-by-layer (LBL) method are advantageous in comparison with those prepared by other methods.<sup>10</sup> The LBL films are uniform visually with a high degree of thickness control. This material shows a globular morphology, which is common in LBL films. The thickness measured with the atomic force microscope (AFM) tip was 25 Å per bilayer.<sup>11</sup> Because the precursors were preformed inorganic and organic polymers, the irreversible reduction of some  $V^{5+}$  sites for the oxidation of aniline (2.33 e<sup>-</sup> for each aniline unit) was avoided. Further advantages were that the amount of PANI distributed within the  $V_2O_5$  matrix could be controlled and the nanocomposite displayed a high charge capacity. In this paper we describe several experiments that reveal new phenomena associated with the nanoarchitecture of layer-by-layer PANI/ $V_2O_5$  films, which is expected to comprise some sort of interpenetrating network. We investigate their electrochemical and electrochromic properties and then show how the electrochemical properties may be affected by adsorbing a PANI/ $V_2O_5$  LBL film on a cast PANI film. As will be seen, the multilayer material shows chromogenic properties of PANI within an oxide matrix with high charge capacity. Moreover, this multilayer structure is able to regulate the ionic transport in PANI as a function of time.

## Experimental Section

$V_2O_5$  was synthesized by following a sol-gel method described in the literature.<sup>12</sup> Briefly, 0.2 mL of vanadyl tri(isopropoxide),  $VC_3H_7O_4$  (Gelest), was added to 100 mL of pure water. The yellowish liquid obtained was evaporated by heating in a vacuum at 70 °C. This procedure was interrupted when the concentration of  $V_2O_5$  reached 0.04 M. The emeraldine base form of PANI was chemically synthesized using the method proposed by Mattoso et al.<sup>13</sup> We followed the procedures by Cheung et al. to prepare water soluble PANI, with PANI being dissolved in dimethylacetamide (DMAc) solution, and after filtering, HCl was slowly added until the pH was 2.0.<sup>14</sup> The filtering procedure retains the longest chains of PANI. Layer-by-layer (LBL) films of  $V_2O_5$  and PANI were produced by the alternating immersion for 3 min of an indium-tin oxide (ITO,  $In_x[Sn_x]O_{3-y}$ , one side coated on glass by Delta Technologies, sheet resistance  $\leq 20 \Omega$ ) with a geometrical area of 1 cm<sup>2</sup> into the polycationic (PANI) and the polyanionic ( $V_2O_5$ ) dispersions. After each deposition, the substrates were rinsed for 1 min in HCl solution (pH = 2) and dried under a nitrogen flow. LBL films of  $V_2O_5$ /PANI also were produced on cast films from PANI deposited on quartz crystals.

For electrochemical experiments, the counter electrode was a platinum sheet with an area of 10 cm<sup>2</sup>. The quasireference

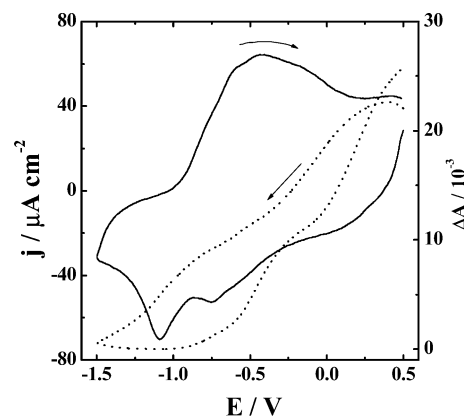


**Figure 1.** Potentiodynamic profiles of current density (—) and absorbance change at 660 nm (---) for 10 bilayers of PANI/ $V_2O_5$ .  $\nu = 20 \text{ mV s}^{-1}$ .

electrode was saturated Ag/AgNO<sub>3</sub>. An electrolytic solution of 0.5 M LiClO<sub>4</sub> (Aldrich) in propylene carbonate (PC) (Aldrich) was used in all experiments. Electrochemical impedance spectroscopy (EIS) experiments were carried out using an ac voltage of 5 mV between 6 mHz and 100 kHz. Chromogenic analysis was made simultaneously with electrochemical experiments using a microprocessor-controlled solid-state light source (WPI, Inc.). Plastic fiber optic cables up to 1 mm in diameter were used to deliver red light (660 nm) from the instrument to a PDA1 photodiode amplifier (WPI, Inc.). These experiments were carried out with an Autolab PGSTAT30. For electrochemical quartz crystal microbalance (EQCM) experiments, the substrates were 6 MHz AT-cut quartz crystal coated with gold using thermal vacuum deposition; a piezoelectric active area of 0.31 cm<sup>2</sup> was used. Only one gold face (working electrode) was exposed to the electrolyte solutions. The resonance frequency shift was measured with a HP-5370B universal time counter. The latter measurements were made with a FAC 2001 potentiostat/galvanostat. Changes in the resonance frequency of the EQCM crystal were transformed into mass changes using the Sauerbrey equation ( $\Delta f = -K\Delta m$ ),<sup>15</sup> where the integral sensitivity constant ( $K = 6.45 \times 10^7 \text{ cm}^2 \text{ s}^{-1} \text{ g}^{-1}$ ) was obtained by calibration using silver electrodeposition.<sup>16</sup>

## Results and Discussion

Figure 1 displays cyclic voltammograms and absorbance changes ( $\Delta A$ ) for 10-bilayer LBL films of  $V_2O_5$ /PANI, obtained with a sweeping rate of 20 mV s<sup>-1</sup>. The  $\Delta A$  values were calculated from the transmittance ( $\Delta A = \log 1/T$ ) and obtained in situ during the intercalation/deintercalation process of lithium ions at a wavelength of 660 nm. The voltammetric profile is similar to the published data.<sup>5</sup> However, a marked difference was found between the  $\Delta A$  profiles for this nanocomposite and  $V_2O_5$  xerogel.<sup>10</sup> Electrochromic effects of PANI dominate the potentiodynamic profile of  $\Delta A$  shown in Figure 1, which is associated with the concentration of polarons and bipolarons.<sup>17,18</sup> This  $\Delta A$  behavior indicates a change from emeraldine to leucoemeraldine form during reduction and the converse process during oxidation. The results in Figure 1 also indicate that PANI

(10) Ferreira, M.; Huguenin, F.; Zucolotto, V.; da Silva, J. E. P.; de Torresi, S. I. C.; Temperini, M. L. A.; Torresi, R. M.; Oliveira, O. N. *J. Phys. Chem. B* **2003**, *107*, 8351.

(11) Ferreira, F.; Zucolotto, V.; Huguenin, F.; Torresi, R. M.; Oliveira, O. N. *J. Nanosci. Nanotech.* **2002**, *2*, 29.

(12) Livage, J. *Chem. Mater.* **1991**, *3*, 578.

(13) Mattoso, L. H. C.; MacDiarmid, A. G.; Epstein, A. J. *Synth. Met.* **1994**, *68*, 1.

(14) Cheung, J. H.; Stockton, W. B.; Rubner, M. F. *Macromolecules* **1997**, *30*, 2712.

(15) Sauerbrey, G. *Z. Phys.* **1959**, *155*, 206.

(16) Gabrielli, C.; Keddam, M.; Torresi, R. M. *J. Electrochem. Soc.* **1991**, *138*, 2657.

(17) Genies, E. M.; Lapkowski, M. *J. Electroanal. Chem.* **1987**, *220*, 67.

(18) Malta, M.; Gonzalez, E. R.; Torresi, R. M. *Polymer* **2002**, *43*, 5895.

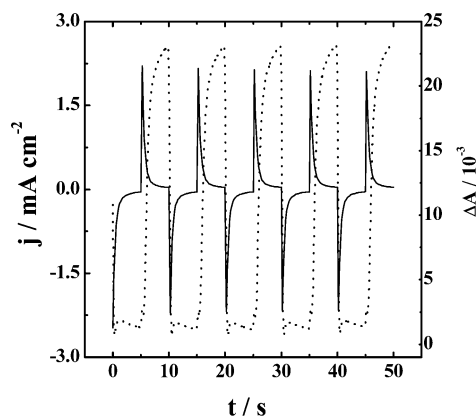


**Figure 2.** Chronoamperometric profiles of current density (—) and absorbance change at 660 nm (---) for 10 bilayers of PANI/ $V_2O_5$ . The potential applied was  $-1.5$  and  $0.5$  V for  $5$  s.

participates in the redox process in the whole range of applied potentials. Taken together, the data in Figure 1 point to a nanocomposite material with the chromogenic properties of PANI and the electrochemical profile of  $V_2O_5$ . Despite the high absorption coefficient and charge capacity of PANI and  $V_2O_5$ , respectively, these characteristics had not been observed for  $V_2O_5$ /PANI nanocomposites obtained using other preparation methods, probably because the interaction can decrease the PANI electroactivity.<sup>5,19</sup> In contrast, the LBL method allows control of the fraction of electrochemically active PANI within the  $V_2O_5$  matrix. It is known from UV-vis and Raman experiments that the fraction of pernigraniline PANI increases as a function of the number of bilayers,<sup>10</sup> because of electronic transfer from emeraldine PANI to  $V_2O_5$  at their interface. With a small number of layers, the excess of oxidized PANI can be avoided and a large amount of emeraldine PANI may participate in the electrochromic process. This hypothesis is consistent with the slope of the decrease in absorbance change as a function of the charge injected, which is  $4.81$ ,  $2.36$ , and  $2.08$   $C^{-1}$  for  $10$ -,  $15$ -, and  $20$ -bilayer LBL films.

Films from  $V_2O_5$  or PANI have been studied for electrochromic devices.<sup>12,18</sup> It was interesting therefore to perform chronoamperometric and spectroelectrochemical experiments, and Figure 2 shows data obtained at  $-1.5$  and  $0.5$  V for  $5$  s. Analogously to the voltammetric data,  $\Delta A$  values correspond to the electrochromic effects of PANI, with good Coulombic reversibility (97%). For the firsts  $50$  cycles, the  $\Delta A$  profile is invariant with the number of charge/discharge steps, with the charge being  $1.6$   $mC\ cm^{-2}$ .

The electronic conductivity and mobility of  $Li^+$  ions injected into host matrices can be analyzed with impedance spectroscopy. Nyquist diagrams are illustrated in Figure 3 for several dc potentials, viz. (a)  $0.5$ , (b)  $0.3$ , (c)  $0.0$ , (d)  $-0.3$ , (e)  $-0.5$ , (f)  $-0.8$ , (g)  $-1.2$ , and (h)  $-1.4$  V with  $5$  mV of ac amplitude. Figure 3a shows a semicircle associated with the bulk resistance ( $R_b$ ) and the geometrical capacitance of the film. The high  $R_b$  (ca.  $26\ k\Omega\ cm^2$ ) indicates that PANI is oxidized at  $0.5$  V. The  $V_2O_5$  xerogel films also present a high value of bulk resistance at this potential ( $900\ k\Omega\ cm^2$  for a film of  $4$

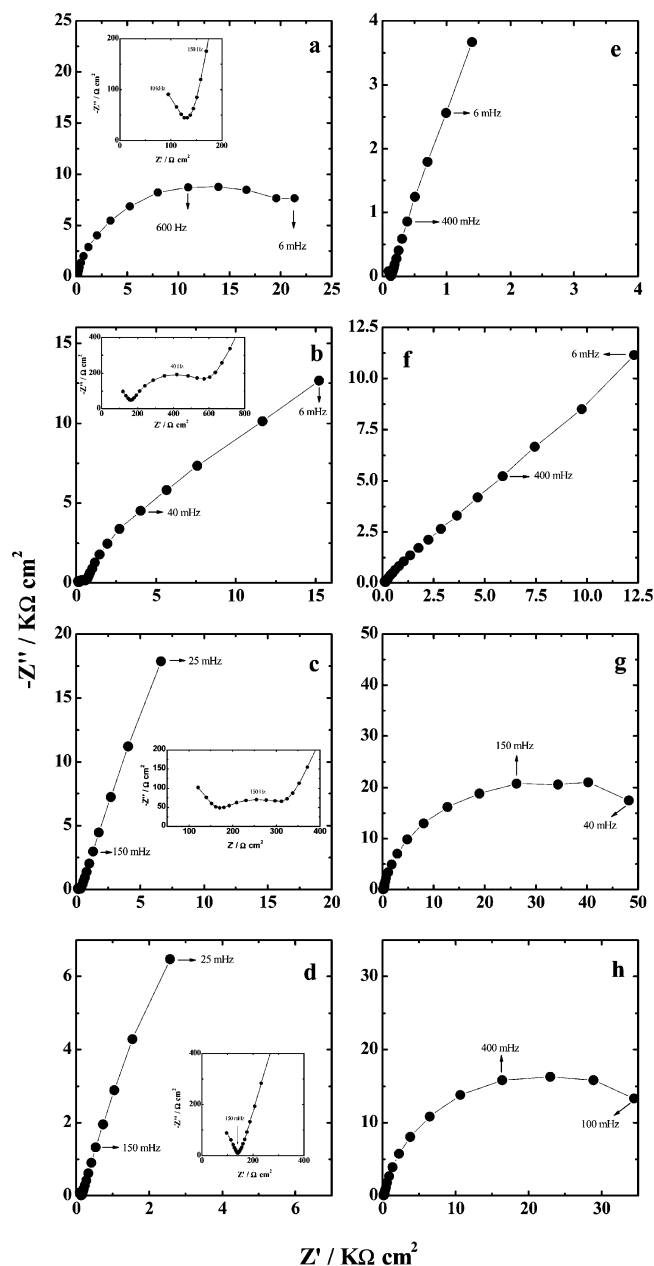


**Figure 3.** Nyquist diagram for 10 bilayers of PANI/ $V_2O_5$  at  $0.5$  V (a),  $0.3$  V (b),  $0.0$  V (c),  $-0.3$  V (d),  $-0.5$  V (e),  $-0.8$  V (f),  $-1.2$  V (g), and  $-1.4$  V (h). The insets show Nyquist diagram for the highest frequencies.

$\mu g\ cm^{-2}$  with a thickness of  $27$  nm and an area of  $1\ cm^2$ ).<sup>4</sup> The inset shows the final part of a semicircle associated with a coupling between the resistance and the geometrical capacitance of the electrolytic solution at the highest frequencies. Interestingly, Figure 3b displays two processes, the first of which shown in the inset (semicircle observed between  $10\ kHz$  and  $150\ Hz$ ) is associated with the electronic transport in a phase that is more conducting than the phase observed at low frequencies. The resistance ( $R_c$ ) of the more conducting phase is  $510\ \Omega\ cm^2$ . As can be seen in the insets of Figure 3c,d, the resistance of the more conducting phase decreases for more negative potentials ( $R_c$  is  $210\ \Omega\ cm^2$  at  $0.0$  V and it is not visualized in the Nyquist diagram for  $-0.3$  V). Thus, we believe that this more conducting phase is formed from emeraldine PANI and  $V_2O_5$ , particularly because the resistance of  $V_2O_5$  decreases

(19) Oliveira, H. P.; Graeff, C. F. O.; Brunello, C. A.; Guerra, E. M. *J. Non-Cryst. Solids* **2000**, *273*, 193.

when  $V^{5+}$  is partially reduced to  $V^{4+}$ .<sup>20</sup> On the other hand, the more insulating phase most likely contains pernigraniline PANI, since PANI has a higher resistance than  $V_2O_5$  for this potential range.<sup>4,21</sup> Figure 3a,b shows a decrease in  $R_b$  as the potential is changed from 0.5 to 0.3 V. This resistance behavior appears to be closely connected with the partial reduction of pernigraniline.

The frequency range associated with the electronic transport in the more insulating phase is near that characteristic of diffusion of lithium ions (Figure 3c–e).<sup>5</sup> However, the impedance is lower in the diffusion process. As these processes occur in parallel within the nanocomposite, the finite diffusion process (saturation charge) is observed at the lowest frequencies, which is characterized by a capacitive-like behavior. A small departure from the ideal behavior can be interpreted as arising from electronic migration effects in the more insulating phase. Another feature is the straight line at low frequencies in Figure 3f, which has a slope of ca.  $45^\circ$  with the  $x$ -axis, indicating a semi-infinite diffusion process of lithium ions ( $D = 10^{-8}$ – $10^{-12}$   $\text{cm}^2 \text{ s}^{-1}$ ).<sup>4,5,22</sup> This means that the ionic diffusion rate decreased with increasing injected charge in the nanocomposite film.<sup>22</sup> The mobility of  $\text{Li}^+$  decreases with increasing concentration of  $\text{Li}^+$  into the film due to  $\text{Li}^+ \cdots \text{Li}^+$  interactions in the host structure.

Figure 3g,h shows only one semicircle, which is attributed to the electronic migration process in the nanocomposite.<sup>23</sup> The excess of  $V^{4+}$  sites in comparison to  $V^{5+}$  sites and the presence of leucoemeraldine PANI tend to increase the electronic resistance of the material at  $-1.2$  V.<sup>5</sup> However, a decrease in resistance is observed from  $-1.2$  to  $-1.4$  V (from ca. 60 to ca. 42  $\text{k}\Omega \text{ cm}^2$ , respectively), indicating that a fraction of PANI oxidized is reduced to a more conducting form (emeraldine). The decrease in resistance is attributed to the reduction of pernigraniline in the more insulating phase, increasing PANI conductivity. This is the reason for  $E < -1.0$  V; the current density in the voltammograms is higher for these nanocomposites than for  $V_2O_5$  xerogel (40 and 12  $\mu\text{A cm}^{-2}$ , respectively).<sup>2,10</sup> The incomplete reduction of PANI for  $E > -1.0$  V is probably associated with highly resistive paths, such as those surrounded by oxide chains. These impedance results help to explain the good electrochemical performance of the cathodes formed from PANI/ $V_2O_5$ . The presence of a conducting path for the whole potential range facilitates the access of ions and electrons to the oxide matrix, since the electronic resistance of  $V_2O_5$  is high for more negative potentials.

The electrochemical properties indicate that  $V_2O_5$ /PANI LBL nanocomposites can be used in lithium batteries. However, useful applications require the mass of the cathodes to be much higher than for a LBL film. We have therefore tested the possibility of adsorbing an LBL film on a much thicker, cast PANI film. The various

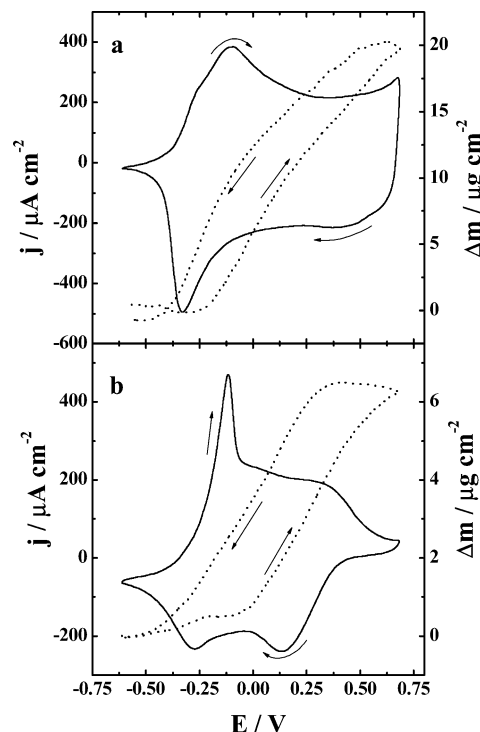


**Figure 4.** Potentiodynamic profiles of current density (—) and mass change (---) as a function of immersion time for PANI: (a) as-immersed and (b) immersed for 24 h into the electrolytic solution.  $v = 20 \text{ mVs}^{-1}$ .

electrochemical studies indicate excellent performance for this specially designed cathode, as we now show. First, to analyze the voltammetric profile and determine the charge compensation process for the cathode, EQCM experiments were carried out for a cast PANI film, in which the potentiodynamic profile of current density and mass shift ( $\Delta m$ ) were obtained as a function of the immersion time of PANI into the electrolytic solution. Figure 4 illustrates the EQCM data for the cast PANI film (a) as-immersed and (b) after 24 h immersion into the electrolytic solution. The cyclic voltammetric data show reduction/oxidation over the range from 0.5 to  $-1.5$  V on the negative-going/positive-going scan. A continued  $\Delta m$  decrease/increase occurs on the negative/positive potential scan. The results are similar to the data in the literature<sup>24</sup> and suggest charge compensation via  $\text{ClO}_4^-$  deintercalation/intercalation. However, there are differences between the values in parts a and b in Figure 4 that are not associated with the number of cycles but rather with the long immersion time in the electrolytic solution. In fact, the voltammetric cycle does not change with time. The redox pair at more positive potentials is shifted, as illustrated by the voltammetric peak at 0.37 V being shifted to 0.13 V. This means that the over-oxidation of PANI (from emeraldine to pernigraniline) occurs for more negative potentials when PANI is immersed into the electrolytic solution for 24 h, due to the low stability of the short polymeric chains. Moreover, the charge compensation mechanism is also changed after 24 h of immersion. Assuming that for each electron injected into PANI, one  $\text{ClO}_4^-$  is deintercalated to compensate for the charge, the theoretical value of

(20) Bullot, J.; Cordier, P.; Gallais, O.; Gauthier, M.; Livage, J. *J. Non-Cryst. Solids* **1984**, *68*, 123.

(21) Paul, E. W.; Ricco, A. J.; Wrighton, M. S. *J. Phys. Chem.* **1985**, *89*, 1441.

(22) Baddour, R.; Pereira-Ramos, J. P.; Messina, R.; Perichon, J. *J. Electroanal. Chem.* **1991**, *314*, 81.

(23) Anaissi, F. J.; Demets, G. J. F.; Toma, H. E. *Electrochem. Commun.* **1999**, *1*, 332.

(24) Daifuku, H.; Kawagoe, T.; Yamamoto, N.; Ohsaka, T.; Oyama, N. *J. Electroanal. Chem.* **1989**, *274*, 313.

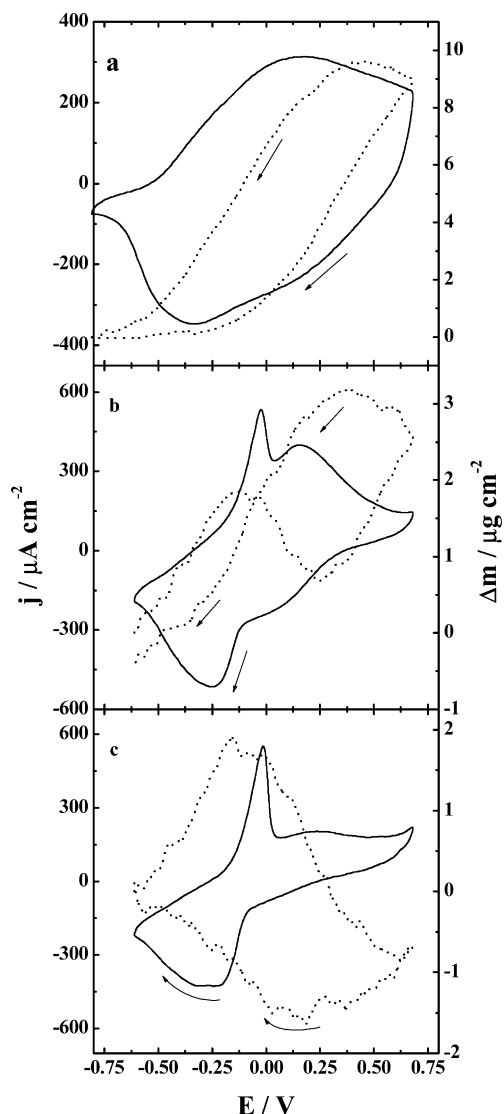


**Figure 5.** Potentiodynamic profiles of current density (—) and mass change (---) as a function of immersion time for nano-composite/PANI: (a) as-immersed, (b) immersed for 12 h and (c) immersed for 24 h into the electrolytic solution.  $v = 20 \text{ mV s}^{-1}$ .

$\Delta m/q$  should be  $1.03 \text{ mg C}^{-1}$ . The experimental values estimated from Figure 4a,b were  $1.69$  and  $0.94 \text{ mg C}^{-1}$ . This difference is associated with the direction of PC flux on intercalation/deintercalation of  $\text{ClO}_4^-$  ions. For the first case (Figure 4a), the direction of PC flux is the same as that of  $\text{ClO}_4^-$  ions. After 24 h in the electrolytic solution, PC molecules intercalate/deintercalate when  $\text{ClO}_4^-$  ions deintercalate/intercalate from the film (Figure 4b).

Figure 5 shows the EQCM data for 10-bilayer  $V_2O_5$ /PANI LBL films deposited on the cast PANI film with the same mass used above ( $118 \mu\text{g cm}^{-2}$ ). The potentiodynamic profile of current density and mass shift are also studied for this cathode as a function of the immersion time into the electrolytic solution: (a) as-immersed, (b) after 12 h, and (c) after 24 h. There is a marked influence from the LBL film on the voltammograms of PANI, which is ascribed to the oxidation of PANI due to  $V_2O_5$ . The chemical instability of PANI short chains also contributes to this oxidation.<sup>25</sup> In fact, the current density at more positive potentials decreases

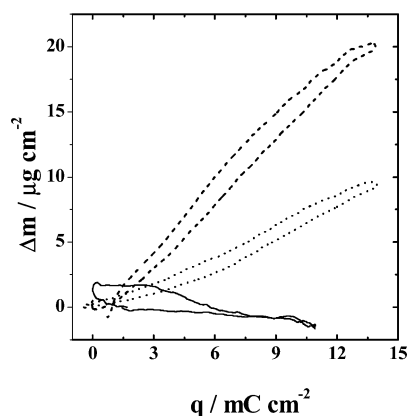


**Figure 6.** Plot of mass change as a function of charge injected for cast PANI as-immersed (---) and for LBL PANI/ $V_2O_5$  film adsorbed on cast PANI as immersed (···) and after 24 h immersion into the electrolytic solution (—).  $v = 20 \text{ mVs}^{-1}$ .

as a function of the immersion time due to the increase in resistance caused by PANI oxidation. We shall resume this discussion below in the analysis of the impedance data. It should be mentioned that these studies could be carried out with the deposition of a cast  $V_2O_5$  xerogel film on the PANI film. If the relative concentration of PANI and  $V_2O_5$  is the same in the cast and LBL films, the voltammetric profile would be similar to that shown in Figure 5. However, the LBL technique allows better control of film thickness than the casting method.

The major features to notice in Figure 5 are the charge compensation changes. The mass gain during the positive-going scan decreases as a function of immersion time, suggesting that the charge compensation process occurs via  $\text{Li}^+$  ions after 24 h. The slope of the  $\Delta m$  values vs charge injected for cast PANI and LBL film adsorbed on PANI (as immersed and after 24 h of immersion into the electrolytic solution) is given in Figure 6. It shifted from  $0.77$  to  $-0.12 \text{ mg C}^{-1}$  when a 10-bilayer LBL film was deposited on the cast PANI film. Assuming that for each electron injected to the cathode, one  $\text{Li}^+$  is intercalated to compensate for the charge, the theoretical value of  $\Delta m/q$  should be  $-0.07 \text{ mg C}^{-1}$ . The difference between experimental ( $-0.12 \text{ mg C}^{-1}$ ) and theoretical ( $-0.07 \text{ mg C}^{-1}$ ) values arises from the contribution from solvent molecules. It is clear from these results that the nanocomposite serves as a filter, which avoids the intercalation/deintercalation from anions into PANI. This means that the charge compensation into  $V_2O_5$ /PANI nanocomposite is effected by  $\text{Li}^+$  ions. As the buildup of these nanoarchitectures results in oxidized PANI (cationic) and reduced  $V_2O_5$  (anionic), the electroneutrality condition is satisfied by the intimate contact between the components. Despite PANI participating in the redox process, its close proximity with  $V_2O_5$  precludes the approach of  $\text{ClO}_4^-$  during oxidation of the polymer chains.<sup>8</sup> This decrease in anionic participation has good implications for the development of lithium secondary batteries with high charge capacity.<sup>26</sup> Other significant advantages of the LBL method are

(25) Rodríguez, J.; Grande, H.-J.; Otero, T. F. *Handbook of Organic Conductive Molecules and Polymers*; John Wiley & Sons: Chichester, 1997; p 415.

(26) Varela, H.; Huguenin, F.; Malta, M.; Torresi, R. M. *Quim. Nova* **2002**, 25, 287.

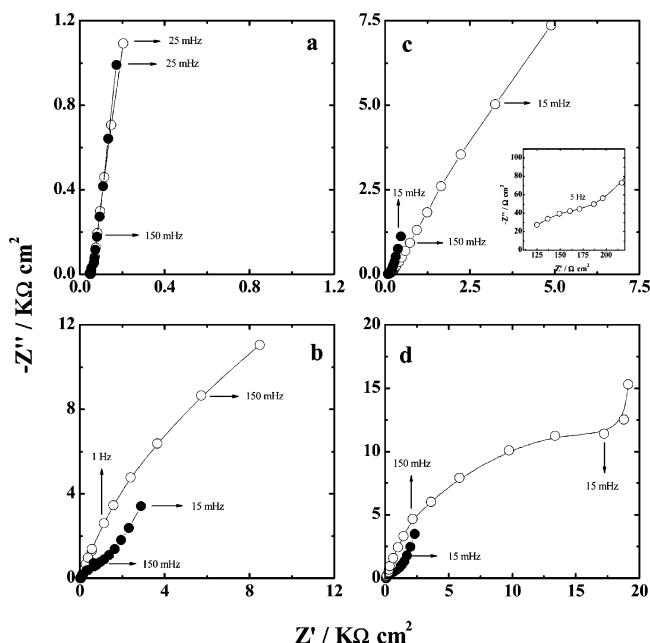


**Figure 7.** Nyquist diagram at 0.6 V (○) and 0.0 V (●) for PANI as immersed (a) and after immersed for 24 h into the electrolytic solution (b). Nyquist diagram at 0.6 V (○) and 0.0 V (●) for the LBL PANI/V<sub>2</sub>O<sub>5</sub> film adsorbed on cast PANI as immersed (c) and after 24 h immersion into the electrolytic solution (d). The inset shows Nyquist diagrams for the highest frequencies.

inferred from these results. By controlling composition, molecular architecture, and immersion time, it is possible to obtain the intercalation/deintercalation of desired ionic species into the host matrix.

Figure 7a shows similar Nyquist diagrams for the cast PANI film as immersed into the electrolytic solution at 0.6 and 0.0 V. The capacitive behavior indicates a saturation charge into conducting PANI (emeraldine form). Electronic transport in the impedance data for the PANI cast film cannot be observed because of the high conductivity of emeraldine. Nyquist diagrams for PANI after 24 h immersion into the electrolytic solution at 0.6 and 0.0 V are shown in Figure 7b. In contrast to Figure 7a, the beginning of a semicircle is observed at 0.6 V, which indicates an  $R_b$  increase of the PANI film. This means that PANI was oxidized after 24 h immersion into the electrolytic solution. We ascribe this overoxidation to the low chemical stability of the short polymeric chains. Despite the decrease in bulk resistance as the potential is shifted from 0.6 to 0.0 V,  $R_b$  is still larger than in Figure 7a. Figure 7c shows Nyquist diagrams obtained for a 10-bilayer LBL PANI/V<sub>2</sub>O<sub>5</sub> adsorbed onto the cast PANI film as immersed into the electrolytic solution at 0.6 and 0.0 V. Similarly to Figure 7b, the beginning of a semicircle appears at 0.6 V. The high impedance data demonstrate the influence of V<sub>2</sub>O<sub>5</sub> on PANI overoxidation. However, in agreement with the hypothesis from two phases mentioned earlier for the nanocomposite, a more-conducting phase is also observed for this material (see the inset). The  $R_b$  value decreases significantly as the potential is shifted from 0.6 to 0.0 V owing to the change from pernigraniline to emeraldine form. Figure 7d shows Nyquist diagrams obtained for the LBL film adsorbed on cast PANI film after 24 h immersion in the electrolytic solution at 0.6 and 0.0 V. In addition to the presence of V<sub>2</sub>O<sub>5</sub>, the low

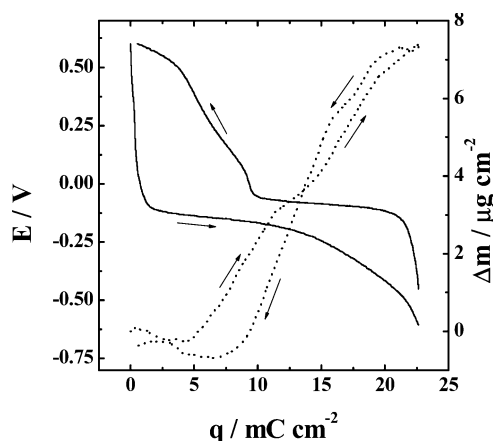


**Figure 8.** Chronopotentiometric curves and profile of mass change for nanocomposite/PANI at 20  $\mu\text{A cm}^{-2}$ .

chemical stability of the short chains contributes to PANI overoxidation, with an increase in bulk resistance in comparison with Figure 7c.

Figure 8 displays the chronopotentiometric curve and the profile of mass change for 130  $\mu\text{g cm}^{-2}$  from the LBL film adsorbed on PANI after 24 h immersion into an electrolytic solution. The current density employed was 20  $\mu\text{A}$  and the geometrical area used was 0.31  $\text{cm}^2$ . The  $\Delta m$  vs  $q$  slope is ca.  $-0.44 \text{ mg C}^{-1}$ , which indicates the participation of lithium ions and solvent molecules in the charge compensation process. Despite the high Ohmic drop for more positive potentials, which is attributed to PANI overoxidation, the charge capacity (48 A h  $\text{kg}^{-1}$ ) was considered satisfactory in comparison with the PANI (100 A h  $\text{kg}^{-1}$ ) and self-doped PANI (44 A h  $\text{kg}^{-1}$ ) films.<sup>27,28</sup> In fact, as the charge compensation process is performed by  $\text{Li}^+$  ions (and not anions), the specific capacity of a lithium secondary battery is increased due to the decrease in the amount of electrolyte.

## Conclusions

Electrochromic multilayer materials were produced from V<sub>2</sub>O<sub>5</sub> and PANI with the layer-by-layer method, where control of thickness and charge capacity could be achieved. Manipulations on the nanometric scale allowed the chromogenic properties of PANI to be obtained while the electrochemical profile of V<sub>2</sub>O<sub>5</sub> xerogel was maintained. Interactions between V<sub>2</sub>O<sub>5</sub> and PANI promoted the formation of two phases. The more conducting phase is formed from V<sub>2</sub>O<sub>5</sub> and emeraldine PANI, while the more insulating one comprises pernigraniline PANI. The former phase becomes insulating for more negative potentials, and pernigraniline is changed to a more conducting PANI. Thus, PANI contributes as a conducting and electroactive polymer in the whole range of potentials. Another advantage of the LBL film is the participation of lithium ions in the charge compensation process, which decreases the mass and may increase the specific capacity of lithium secondary batteries. In addition, the ionic flux into the PANI film can be monitored. The deposition of an LBL

(27) Novák, P.; Müller, K.; Santhanam, K. S. V.; Haas, O. *Chem. Rev.* **1997**, *97*, 207.

(28) Barbero, C.; Miras, M. C.; Kötz, R.; Haas, O. *Synth. Met.* **1993**, *55*, 1539.

PANI/V<sub>2</sub>O<sub>5</sub> film on a cast PANI film modifies the charge compensation mechanism, which is a function of immersion time of the electrode into the electrolytic solution. This work thus demonstrates the potential of the designed nanocomposites for sensors, electrochromic devices, and lithium secondary batteries.

**Acknowledgment.** Financial assistance from FAPESP and CNPq (Brazil) is gratefully acknowledged. F.H., M.F., and V.Z. thank FAPESP for fellowships.

CM035171S